NJC

ROYAL SOCIETY OF CHEMISTRY

PERSPECTIVE

View Article Online
View Journal | View Issue

Cite this: *New J. Chem.*, 2025, **49**, 6091

T-type diarylethenes for molecular solar thermal energy storage: aromaticity as a design principle

Thillaiarasi Sukumar, [a] D. Sravanakumar Perumalla,[b] Kamatham Narayanaswamy,[a] Bo Durbeej *[b] and Baswanth Oruganti *[ac]

Received 19th December 2024,
Accepted 12th March 2025

DOI: 10.1039/d4nj05407e

rsc.li/njc

Molecular photoswitches that absorb sunlight and store it in the form of chemical energy are attractive for applications in molecular solar thermal energy storage (MOST) systems. Typically, these systems utilize the absorbed energy to photoisomerize into a metastable form, which acts as an energy reservoir. Diarylethenes featuring aromatic ethene π-linkers have garnered research interest in recent years as a promising class of T-type photoswitches, which undergo photocyclization from an aromatic ring-open form into a less aromatic or non-aromatic ring-closed form. Based on several recent computational and experimental studies, this perspective analyzes the potential of these switches for MOST applications. Specifically, we discuss how they can be made to simultaneously achieve high energy-storage densities, long energy-storage times, and high photocyclization quantum yields by tuning the aromatic character of the ethene π-linker.

Introduction

Solar energy is an inexhaustible and environmentally benign renewable energy source that is offering a potential solution to the global energy crisis. However, the availability of solar energy is hindered by geographical location, weather conditions, seasonal variations, and the time of day, which exacerbate the need for developing solar energy storage solutions. Beyond established technologies such as batteries[1] and power-to-X[2] systems, an alternative approach for storing solar energy involves the use of molecular photoswitches. These are typically small organic molecules, which absorb light within the UV or visible region and harness the absorbed energy to undergo isomerization from a low-energy stable form into a high-energy metastable form. When the energy subsequently is needed, the metastable isomer is reverted back to its parent form through a thermal back reaction, which releases the stored energy as heat and may also be induced by heat,[3–5] a catalyst,[6–8] or through chemical or electrochemical stimuli.[9,10] The difference in free energy between the two isomeric forms (ΔG_r) quantifies the energy-storage potential, while the free-energy barrier ($\Delta G_b^{\ddagger}$) for the thermal back reaction determines for how long the energy

[a] *Department of Chemistry, SRM University-AP, Mangalagiri, Andhra Pradesh 522240, India*
[b] *Division of Theoretical Chemistry, IFM, Linköping University, SE-58183 Linköping, Sweden. E-mail: bodur@ifm.liu.se*
[c] *School of Mathematics and Natural Sciences, Chanakya University, Bengaluru-562165, India. E-mail: baswanth.o@chanakyauniversity.edu.in*

Thillaiarasi Sukumar

Ms Thillaiarasi Sukumar obtained her MSc in Chemistry from PSGR Krishnammal College for Women in Tamil Nadu, India. She is currently pursuing her PhD in Computational Chemistry at SRM University – AP. Her current research focuses on computational studies of molecular solar thermal energy storage systems.

D. Sravanakumar Perumalla

Dr D. Sravanakumar Perumalla received his PhD from Indian Institute of Science, Bangalore in 2020. Following postdoctoral work at IIT Palakkad and Indian Institute of Science, Bangalore, he joined Prof. Bo Durbeej group in Linköping University. His research interests include aromaticity, boron based 2D-materials, molecular motors and switches.

can be stored. Photoswitches of this type are commonly referred to as molecular solar thermal energy storage (MOST) systems.[5,11,12]

An efficient MOST system must fulfill several important criteria,[5,11–17] such as showing a high quantum yield for the photochemical reaction forming the metastable isomer, light absorption in the visible region, a high energy-storage per unit weight (E_s, typically >0.30 MJ kg^{-1}), a moderately large free-energy barrier for the thermal back reaction (typically >100 kJ mol^{-1}), a fast response time for stimulus-induced energy release, and a high fatigue resistance (the ability to switch reversibly for large number of cycles). To date, molecular photoswitches explored for developing MOST systems include stilbene,[18] azobenzene,[19] anthracene (dimerization),[20] dihydroazulene/vinylheptafulvene,[21] norbornadiene/quadricyclane,[22] diarylethene,[23] 1,2-azaborine[24] and fulvalene ruthenium compounds.[25] These molecules undergo photoswitching through reactions such as cycloaddition, *cis–trans* isomerization, or electrocyclization reactions.

Among the various classes of photoswitches considered for developing MOST systems, diarylethenes constitute a well-known family of molecules that switch reversibly between ring-open and ring-closed isomeric forms through electrocyclization and cycloreversion reactions.[23,26,27] In photochemically reversible (P-type) diarylethenes, both reactions occur by absorption of light, typically in the UV or visible region.[23,26–29] The ring-closed form in these systems exhibits high thermal stability even at elevated temperatures due to large cycloreversion barriers.[23,26,27] P-type diarylethenes commonly feature a non-aromatic ethene π-linker, such as perfluorocyclopentene[23,26,27] in P-**Io** or cyclohexene in P-**IIo**,[28,29] as shown in Scheme 1. In contrast, thermally reversible (T-type) diarylethenes undergo electrocyclization photochemically, while their cycloreversion is induced thermally.[30–35] Most T-type diarylethenes developed to date feature a third aromatic unit (commonly known as terarylenes), in the form of an aromatic π-linker connecting the two aryl units,[30–35] such as benzene in T-**Io** as illustrated in Scheme 1. Additionally, they exhibit low photocycloreversion quantum yields[36–38] and modest thermal cycloreversion barriers.[30–34]

As illustrated in Scheme 2, T-type diarylethenes developed to date can be broadly classified into three categories: diarylbenzenes (DABs),[31–33,39–43] diarylheteroarenes (DAHs),[38,44,45] and diarylbenzoheteroarenes (DABHs).[36–38,46–49] The first two classes feature monocyclic π-linkers such as benzene,[31–33,39–43] pyrazine[45] and thiazole,[38,44] while DABHs contain polycyclic π-linkers such as indole,[47,49] azaindole[46] and benzothiophene.[36–38] In systems with monocyclic π-linkers, the aromaticity of the π-linker is completely lost upon photocyclization. In systems containing polycyclic π-linkers, while the ring directly connected to the diaryl core loses its aromaticity, rings fused to it might gain some aromaticity.[34,49] As a result of complete or partial loss of aromaticity, large positive ΔG_r values are achievable in these systems, which is an appealing aspect for MOST applications.[34,38,49] However, as expected from the Bell–Evans–Polanyi

Kamatham Narayanaswamy

Dr Kamatham Narayanaswamy is currently working as an Assistant Professor in the Department of Chemistry at SRM University – AP in India. He received his PhD degree in Materials Chemistry from CSIR-Indian Institute of Chemical Technology under the supervision of Dr Surya Prakash Singh in 2017. Then he moved to France for his post-doctoral study, at the CNRS-University of Strasbourg, Sorbonne University Pierre and Marie Curie Campus (UPMC) and University of Montpellier from 2017 to 2022. His research interest focuses on the design, synthesis and characterization of new organic functional π-conjugated materials for photonic and energy applications.

Bo Durbeej

Prof. Bo Durbeej received his PhD from Uppsala University in 2004. Following postdoctoral work at the University of Sydney and the University of Siena, he held a position at the Swedish Defense Research Agency before joining (in 2010) Linköping University, where he was promoted to Professor in 2019. His recent research interests include molecular motors and switches, photosensory proteins and enzyme catalysis.

Baswanth Oruganti

Dr Baswanth Oruganti is currently working as an Associate Professor in Chemistry at Chanakya University in India. He obtained his PhD in Theoretical Chemistry at Linköping University in Sweden under the guidance of Prof. Bo Durbeej. Subsequently, he pursued post-doctoral research in Computational Biochemistry at Linnaeus University in Sweden. His current research interests include computational photochemistry and quantum computing for chemistry simulations.

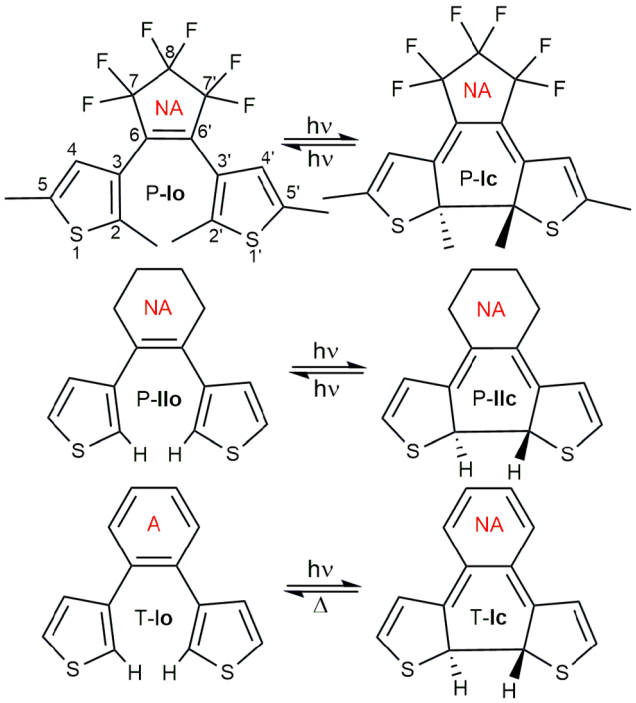

Scheme 1 Isomerization between ring-open (**o**) and ring-closed (**c**) forms of P-type (P-**I** and P-**II**) and T-type (T-**I**) diarylethenes through electrocyclization and cycloreversion reactions. Aromaticity, non-aromaticity and antiaromaticity are abbreviated as A, NA, and AA, respectively.

principle,[50] a large positive ΔG_r for electrocyclization typically leads to a small $\Delta G_b^{\ddagger}$ value for cycloreversion,[31–33,49] resulting in poor thermal stability of the ring-closed form and short energy-storage times.

Several recent studies have identified strategies to modulate the cycloreversion kinetics of DABs,[33,40–43] DAHs[9,38] and DABHs,[38] offering insights into possible ways by which energy-storage times can be improved. As depicted in Scheme 2, strategies targeting chemical modifications of the diaryl core to impede cycloreversion include employing sterically less bulky substituents on the reactive C2 and C2′ atoms[9,38,42,43] or introducing electron-donating groups on phenyl substituents at the lateral C5 and C5′ atoms.[40,43] Furthermore, replacing the conventionally employed dithienyl core (DAB-**I** and DAH-**I**) with less aromatic dithiazolyl core (DAB-**II** and DAH-**II**) increases the half-lives of ring-closed form by several orders of magnitude.[33,38,41] Alternatively, chemical modifications of the π-linker in DABs, involving the replacement of a tetrafluorobenzene (DAB-**II**) with a difluorobenzene (DAB-**III**), was found to increase cycloreversion barriers by up to 14 kJ mol^{-1}.[33,42]

In this perspective, we focus on how tuning the aromaticity of the π-linker enables achieving both large ΔG_r and $\Delta G_b^{\ddagger}$ values simultaneously in T-type diarylethenes containing monocyclic and polycyclic π-linkers. Furthermore, we analyze how electronic excitation modulates aromaticity[51–53] in order to maximize the photochemical reactivity of these systems,[32,34,39,49] which is another key requirement for MOST applications. Additionally, we discuss how the presence of a heteroaromatic unit bearing a nitrogen atom facilitates fast response times in stimulus-induced energy release. Overall, this paper synthesizes insights from several recent computational and experimental studies[31–34,38,39,45,48,49] to formulate strategies for optimizing several MOST criteria simultaneously by using aromaticity as a design principle.

Computational and experimental methods

In the following, we outline the computational protocol employed in our recent studies,[32,34,39,49] which was found to

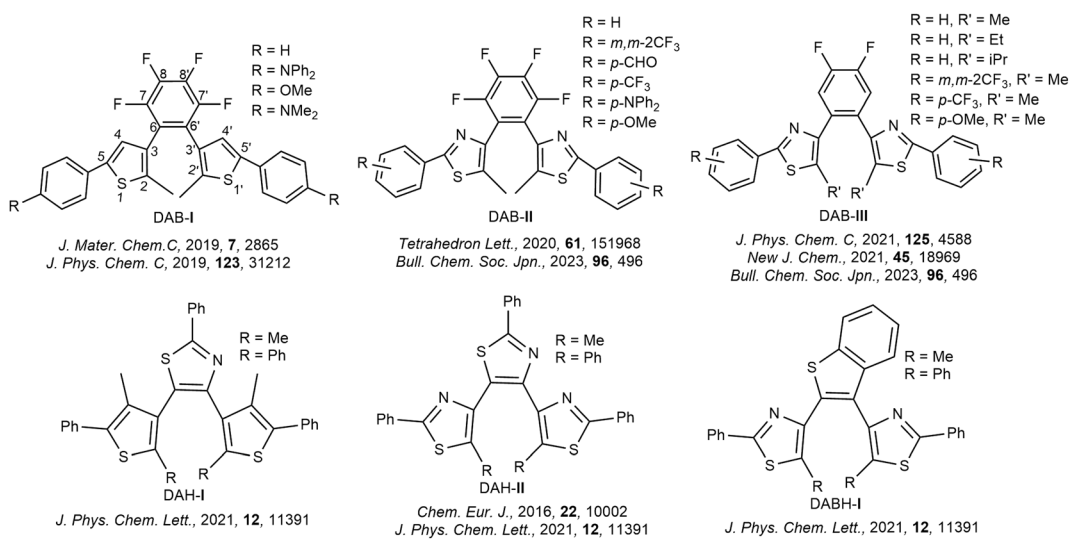

Scheme 2 Structures of the ring-open forms of diarylbenzenes (DAB-**I**, DAB-**II** and DAB-**III**), diarylheteroarenes (DAH-**I** and DAH-**II**), and diarylbenzoheteroarenes (DABH-**I**) considered in previous studies to investigate the influence of steric bulkiness and electronic nature of substituents (R and R′), and effect of aromaticity on kinetics of cycloreversion.

be optimal in terms of efficiency and accuracy for modeling the thermal and photochemical isomerizations of T-type diarylethenes. First, the thermal electrocyclization and cycloreversion reactions of the switches were investigated by calculating reaction free energies and free-energy barriers by using hybrid density functionals in combination with the SMD solvation model.[54] Subsequently, using time-dependent DFT (TD-DFT)[55] or multi-configurational methods such as CASSCF[56] and CASPT2,[57,58] the photocyclization reactions were explored by calculating reaction paths starting from the vertically excited Franck–Condon (FC) points in the photoactive excited state (typically S_1) of the switches. Along the reaction paths, which typically involve a S_1/S_0 conical intersection seam offering a non-radiative decay channel for the photoexcited species, changes in aromaticity of the π-linker were monitored by computing various aromaticity indices, such as harmonic oscillator model of aromaticity (HOMA),[59] nucleus-independent chemical shift (NICS)[60] and Shannon aromaticity (SA) indices.[61] This helps in rationalizing photocyclization reactivity in terms of photoinduced changes in aromatic character of the π-linker.[51–53] Finally, in order to estimate photocyclization efficiencies and excited-state lifetimes, computationally more demanding non-adiabatic molecular dynamics (NAMD) simulations[32,39,49,62] were carried out for a smaller subset of compounds using TD-DFT/DFT.[63]

Beyond our own studies,[32,34,39,49] several T-type diarylethenes synthesized and characterized by other research groups[31,33,38,45,48] were also considered. In the corresponding studies,[31,33,38,45,48] the associated cycloreversion rate constants were derived from UV-visible measurements. Herein, these rate constants were then transformed into free-energy barriers using standard transition state theory. Furthermore, these rate constants were also used to calculate half-lives ($t_{1/2}$) of the ring-closed forms under the assumption that the cycloreversion follows first-order kinetics.

Energy-storage density and thermal cycloreversion

As discussed in the Introduction, diarylethenes containing monocyclic aromatic π-linkers, such as benzene (**1**)[32] and tetrafluorobenzene (**2**),[31] depicted in Scheme 3, achieve large ΔG_r or reaction enthalpies (ΔH_r) of 112–138 kJ mol^{-1}.[31,32] This is because the electrocyclization alleviates the aromaticity of the π-linker by transforming the low-energy (aromatic) ring-open form (**1o** and **2o**) into the high-energy (non-aromatic) ring-closed form (**1c** and **2c**). However, the resulting species is susceptible to thermal cycloreversion, which restores the aromaticity of the π-linker. This is evident from relatively modest $\Delta G_b^{\ddagger}$ values of 60–72 kJ mol^{-1}, reported by two independent combined experimental and computational investigations for these systems.[31,32] To address this challenge, previous studies on diarylethenes featuring monocyclic aromatic π-linkers (Scheme 3a) focused on reducing the aromaticity of the π-linker in the ring-open form of the switch. Specifically, by employing π-linkers that are less aromatic than benzene, such as pyrazine (**3**)[45] and thiazole (**4** and **5**),[38] substantially longer half-lives of ring-closed forms were observed[38,45] due to relatively larger $\Delta G_b^{\ddagger}$ values of 83–106 kJ mol^{-1}, as can be noted from Table 1. Interestingly, modifying the diaryl core from dithienyl in **4** and **5** into dithiazolyl in **6** and **7** increased activation energies (E_a) considerably (by 20–67 kJ mol^{-1}),[38] albeit changes in $\Delta G_b^{\ddagger}$ values are relatively smaller.

Given that the dithienyl core in **1**, **3** and **4** bears identical substituents on the reactive C2 and C2′ atoms (see Scheme 3a), it is possible that the increase in $\Delta G_b^{\ddagger}$ values of switches **3** and **4** relative to **1** stems primarily from changes in aromaticity of the π-linker. As illustrated in Fig. 1, it can be hypothesized that the transition structures (TSs) mediating the thermal cycloreversion of **3** and **4** experience a destabilization relative to the TS of **1** due to a decreased aromaticity of the π-linker, without any concomitant effect in the ring-closed form. This is because π-linker is non-aromatic in the ring-closed forms of all the three switches. Furthermore, the ring-open forms of **3** and **4** also experience destabilization, relative to that of **1**, due to lowered aromaticity of the π-linker. Indeed, a small ΔH_r value of ∼71 kJ mol^{-1} observed for **4**,[38] supports this hypothesis.

In our recent computational work,[49] we have demonstrated an alternative design strategy to enhance the thermal stability of the ring-closed form of diarylethenes that involves increasing the aromaticity of its π-linker.[49] Specifically, by employing polycyclic π-linkers containing a heteroarene unit fused to a benzenoid ring in the ring-open form of the switch, it was ensured that the ring-closed form also retains the appended aromatic unit.[49] To evaluate the cycloreversion reactivity of resulting DABH switches with multiple aromatic rings, a suitable reference system constitutes a switch containing a π-linker with a non-aromatic unit fused to the benzene ring, such as indene in **9**. Expectedly, the $\Delta G_b^{\ddagger}$ value of 61–64 kJ mol^{-1} for the dithienylindene switch **9**[49] is close to the corresponding 67–71 kJ mol^{-1} value for the dithienylbenzene switch T-**I**,[32] suggesting that the appended non-aromatic cyclopentadiene unit has minimal impact on cycloreversion reactivity. Thus, **9** serves as a suitable reference system to assess how replacing its non-aromatic cyclopentadiene unit with an aromatic pyrrole unit, such as in dithienylindole (**10**) and dithienylisoindole (**11**) switches depicted in Scheme 3b, influences the $\Delta G_b^{\ddagger}$ value.

While the electrocyclization reaction annihilates aromaticity of the central benzene ring of the π-linker in all the three switches **9**, **10** and **11**, we envisioned that it might actually accentuate aromaticity of the appended pyrrole unit in **10** and **11**.[49] Consequently, as illustrated in Fig. 2, the ring-closed forms of **10** and **11** are expected to exhibit larger aromaticity-induced stabilization than their ring-open and TS forms, relative to the corresponding species of **9** entailing a non-aromatic cyclopentadiene unit. This effect was quantified by calculating reaction energies for isomerization between an amino-derivative of **9** and methyl derivatives of **10** and **11** for all the three species.[49] These calculations revealed that the aromaticity-induced stabilization in the ring-closed forms of **10** and **11** is 21–24 and 50–55 kJ mol^{-1} larger than in the

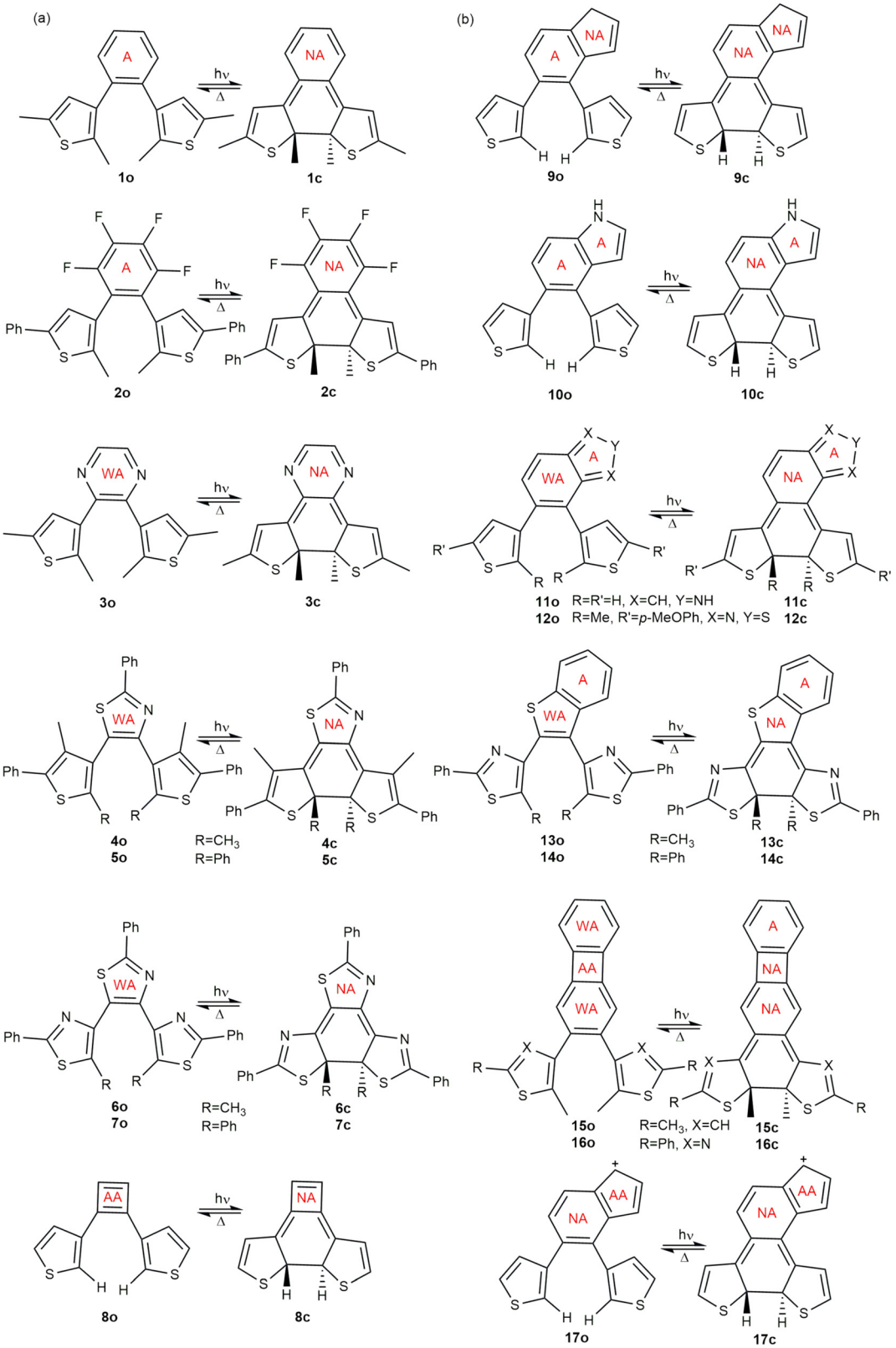

Scheme 3 Structures of the ring-open (**o**) and ring-closed forms (**c**) of diarylethenes featuring (a) monocyclic (**1**, **2**, **3**, **4**, **5**, **6**, **7** and **8**) and (b) polycyclic (**8**, **9**, **10**, **11**, **12**, **13**, **14**, **15**, **16** and **17**) π-linkers. A, WA, NA, and AA represent aromatic, weakly aromatic (relative to benzene), non-aromatic, and antiaromatic, respectively.

Table 1 $\Delta G_b^{\ddagger}$, E_a, ΔG_r, ΔH_r, $t_{1/2}$ and E_s values for diarylethene switches containing monocyclic and polycyclic π-linkers[a]

Switch	Diaryl core	π-Linker	Method	$\Delta G_b^{\ddagger}$ (E_a) [kJ mol^{-1}]	ΔG_r (ΔH_r) [kJ mol^{-1}]	$t_{1/2}$ [s]	E_s [MJ kg^{-1}]
Monocyclic							
T-**I**	Dithienyl	Benzene	B3LYP[b]	71 (—)	112 (-)	3.1×10^{-1}	0.46
			ωB97X-D[b]	67 (—)	123 (—)	6.2×10^{-2}	0.51
1	Dithienyl	Benzene	ωB97X-D[b]	72 (—)	138 (—)	4.7×10^{-1}	0.46
2	Dithienyl	Tetrafluorobenzene	B3LYP[c]	60 (57)	— (111)	3.7×10^{-3}	—
			M06-2X[c]	69 (67)	— (—)	1.3×10^{-1}	—
			Experiment[d]	69 (66)	— (—)	1.3×10^{-1}	—
3	Dithienyl	Pyrazine	Experiment[e]	83 (—)	— (—)	69	—
4	Dithienyl	Thiazole	Experiment[f]	106 (92)	— (71)	1.1×10^{6}	0.13
5	Dithienyl	Thiazole	Experiment[f]	83 (37)	— (—)	58	—
6	Dithiazolyl	Thiazole	Experiment[f]	90 (112)	— (—)	1.2×10^{3}	—
7	Dithiazolyl	Thiazole	Experiment[f]	85 (104)	— (—)	1.4×10^{2}	—
8	Dithienyl	Cyclobutadiene	B3LYP[b]	128 (—)	−24 (—)	3.3×10^{9}	—[k]
Polycyclic							
9	Dithienyl	Indene	B3LYP[g]	64 (—)	118 (—)	1.8×10^{-2}	0.42
			ωB97X-D[g]	61 (—)	130 (—)	5.5×10^{-3}	0.46
10	Dithienyl	Indole	B3LYP[g]	86 (—)	98 (—)	133	0.35
			ωB97X-D[g]	83 (—)	109 (—)	40	0.39
11	Dithienyl	Isoindole	B3LYP[g]	108 (—)	76 (—)	9.5×10^{5}	0.27
			ωB97X-D[g]	113 (—)	79 (—)	7.2×10^{6}	0.28
12	Dithienyl	Benzothiadiazole	Experiment[h]	99 (—)	— (—)	4.6×10^{4}	—
13	Dithiazolyl	Benzothiophene	Experiment[f]	125 (137)	— (25)	2.4×10^{9}	0.05
14	Dithiazolyl	Benzothiophene	Experiment[f]	108 (114)	— (110)	1.8×10^{6}	0.18
15	Dithienyl	Biphenylene	B3LYP[i]	105 (—)	101 (—)	2.7×10^{5}	0.27
16	Dithiazolyl	Biphenylene	B3LYP[i]	105 (105)	90 (—)	3.2×10^{5}	0.24
			Experiment[j]	119 (117)	— (—)	9.7×10^{7}	—
17	Dithienyl	Indenyl cation	B3LYP[g]	61 (—)	2 (—)	5.5×10^{-3}	0.01
			ωB97X-D[g]	54 (—)	16 (—)	3.3×10^{-4}	0.06

[a] "—" indicates unavailability of data. [b] Calculations carried out using the aug-cc-pVTZ basis set and an SMD description of an acetonitrile solvent.[32,34] [c] $\Delta G_b^{\ddagger}$ estimated using the reported E_a values at the B3LYP/6-31G(d) and M06-2X/6-31G(d) levels of theory and the pre-exponential factors taken from UV-visible absorption measurements in an *n*-hexane solvent at 298 K.[31,33] [d] $\Delta G_b^{\ddagger}$ estimated using rate constants from UV-visible absorption measurements in an *n*-hexane solvent at 298 K.[31] [e] $\Delta G_b^{\ddagger}$ estimated using rate constants from UV-visible absorption measurements in a toluene solvent at 293 K.[45] [f] ΔH_r and E_s from differential scanning calorimetry measurements; $\Delta G_b^{\ddagger}$ estimated using rate constants from UV-visible absorption measurements in a toluene solvent at 293 K.[38] [g] Calculations carried out using the cc-pVTZ basis set and an SMD description of an acetonitrile solvent.[49] [h] $\Delta G_b^{\ddagger}$ estimated using rate constants from UV-visible absorption measurements in chloroform solvent at 293 K.[48] [i] Calculations carried out using the cc-pVTZ basis set and an SMD description of a toluene solvent.[34] [j] $\Delta G_b^{\ddagger}$ and $t_{1/2}$ values estimated at 298 K based on activation energy and rate constant values from ^{1}H NMR measurements in C_6D_6 solvent at 343 K (assuming that activation energy is independent of temperature).[34] [k] No energy storage is possible as the ring-closed form is more stable than the ring-open form.[34]

corresponding ring-open and TS forms, respectively.[49] The stabilization of the ring-closed form explains almost quantitatively why the $\Delta G_b^{\ddagger}$ values for **10** and **11** in Table 1 are 22 and 44–52 kJ mol^{-1} larger than those for **9**, while the corresponding ΔG_r values are 20–21 and 42–51 kJ mol^{-1} smaller.[49] Despite the lowering of ΔG_r, **10** and **11** maintain considerable E_s values of 0.27–0.39,[49] making them promising candidates for further development as MOST systems.

Building on our design strategy, we extend the analysis to previously reported DABH switches featuring benzo[*c*]-[1,2,5]-thiadiazole (**12**)[48] and benzothiophene (**13** and **14**) π-linkers.[38] In these switches, the ring-closed forms are expected to be stabilized by the aromaticity of the thiadiazole (**12**) and benzene (**13** and **14**) rings, fused to the central benzene and thiophene moieties, respectively (see Scheme 3b). As a result, their $\Delta G_b^{\ddagger}$ values are predicted to be larger compared to **9**. Switches **13** and **14**, however, benefit from an additional effect: the dithiazolyl core in their π-linkers is less aromatic than the dithienyl core in **9**, which destabilizes the ring-open and TS forms relative to the ring-closed form. This combined effect—stabilization of the ring-closed form and destabilization of the TS—results in larger $\Delta G_b^{\ddagger}$ values for **13** (∼125 kJ mol^{-1})[38] and **14** (∼108 kJ mol^{-1})[38] compared to **12** (∼99 kJ mol^{-1}).[48] These $\Delta G_b^{\ddagger}$ values are substantially larger than the 61–64 kJ mol^{-1} observed for **9**,[49] underscoring broader applicability of our design strategy. Overall, introducing benzoheteroarene π-linkers in diarylethenes facilitates achieving large $\Delta G_b^{\ddagger}$, with only modest compromise on ΔG_r, primarily through aromaticity-induced stabilization of the ring-closed form. These findings are further corroborated by recent studies on a diverse set of diarylethenes featuring bicyclic[64] and tricyclic[65] π-linkers, containing one or more heteroaromatic units fused to the central benzene ring.

In another recent study on diarylethene switches containing a tricyclic weakly aromatic biphenylene π-linker (**15** and **16**),[34] we demonstrated that electrocyclization enhances the aromaticity of the terminal phenyl ring of the biphenylene motif, thereby improving the thermal stability of the ring-closed form. As a result, mimicking the behavior of DABH switches discussed above, switches **15** and **16** also show substantially large $\Delta G_b^{\ddagger}$ values of 105–119 kJ mol^{-1}.[34] Moreover, these switches also show large ΔG_r and E_s values of ∼100 kJ mol^{-1} and 0.24–0.27 MJ kg^{-1},[34] respectively, and thereby appear to be potential candidates for MOST applications. Thus, it can be concluded that while aromaticity of the π-linker in diarylethenes is a

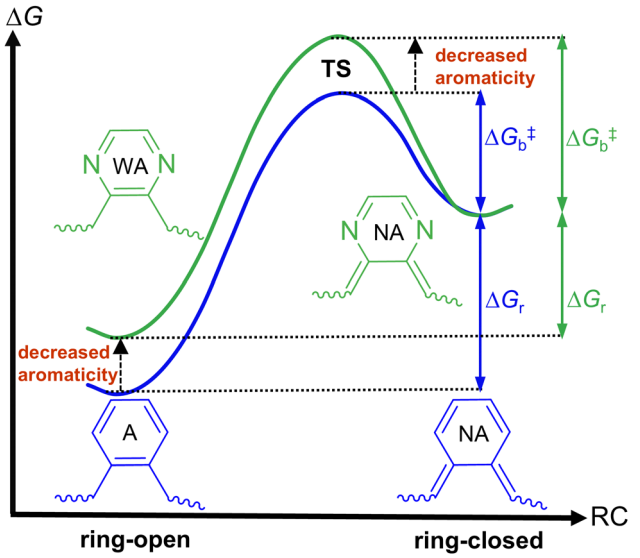

Fig. 1 Schematic illustration of how decreased aromaticity of the pyrazine π-linker (relative to the benzene π-linker) destabilizes the ring-open and TS forms, leading to a smaller ΔG_r and a larger $\Delta G_b^{\ddagger}$. A, WA, and NA denote aromatic, weakly aromatic, and non-aromatic, respectively. Blue and green colors correspond to switches featuring benzene and pyrazine π-linkers, respectively. RC represents the reaction coordinate.

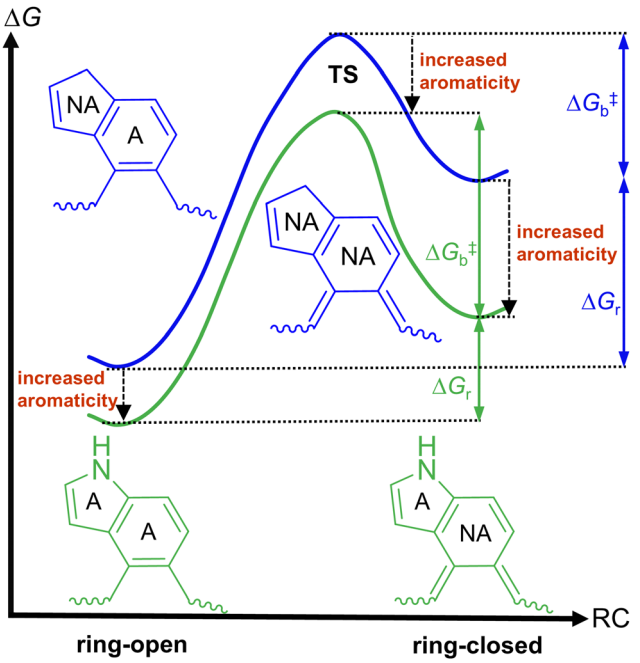

Fig. 2 Schematic illustration of how increased aromaticity of the indole π-linker (relative to the indene π-linker) stabilizes the ring-open, TS and ring-closed forms, leading to a smaller ΔG_r and a larger $\Delta G_b^{\ddagger}$. A, WA, and NA denote aromatic, weakly aromatic, and non-aromatic, respectively. Blue and green colors correspond to switches featuring indene and indole π-linkers, respectively. RC represents the reaction coordinate.

desirable feature for achieving large ΔG_r and E_s values, the degree and distribution of aromaticity are crucial factors that need to be fine-tuned to allow for sufficiently high $\Delta G_b^{\ddagger}$ values.

Photochemical reactivity and fatigue resistance

Having shown that tuning the ground-state aromaticity of the π-linker of diarylethenes is a viable strategy to enhance the energy-storage times of these switches, it is natural then to investigate how the excited-state aromatic character of the π-linker influences the photochemical reactivity. In this regard, our previous studies of diarylethenes with monocyclic aromatic (benzene in **1**)[32,39] and polycyclic heteroaromatic (indole in **10** and isoindole in **11**)[49] π-linkers demonstrated that the π-linker attains antiaromatic character during the initial electronic excitation of these switches. This can be inferred from the change in the sign of the scaled $\langle NICS_{zz} \rangle$ values (from negative to positive) seen in Fig. 3 for the benzene π-linker of **1**, as well as for the indole and isoindole π-linkers of **10** and **11**. Consequently, it was observed that the subsequent relief of excited-state antiaromaticity facilitates fast (200–300 fs) and efficient (60–93%) photocyclization of these switches,[32,39,49] as illustrated in Fig. 4 (panels a, d, and e). Thus, aromatic diarylethenes of this type show a photocyclization efficiency that matches or even surpasses their non-aromatic counterparts featuring ethene-like bridges such as cyclohexene (60%) in P-**Io** (see Scheme 1 and Fig. 4b).[39] On the other hand, diarylethenes featuring antiaromatic π-linkers, be it monocyclic (cyclobutadiene in **8**; see Scheme 3a)[39] or polycyclic (indenyl

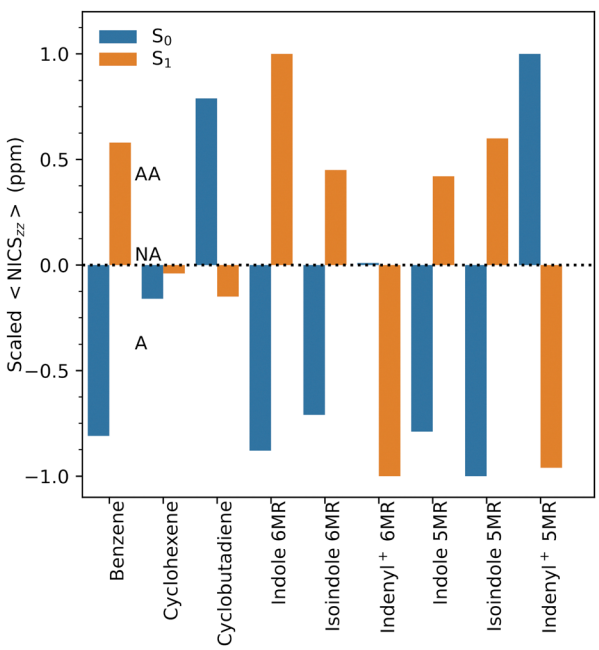

Fig. 3 $\langle NICS_{zz} \rangle$ values of the monocyclic π-linkers benzene (T-**I**), cyclohexene (P-**II**), and cyclobutadiene (**8**); and of the six-membered ring (6MR) and five-membered ring (5MR) of the polycyclic π-linkers indole (**10**), isoindole (**11**), and indenyl cation (**17**) compiled from our previous studies.[32,39,49] To facilitate a balanced comparison between the S_0 and S_1 states, all the $\langle NICS_{zz} \rangle$ values obtained in a given electronic state are scaled between −1 (most aromatic) and +1 (most antiaromatic). Aromaticity, non-aromaticity and antiaromaticity are abbreviated as A, NA, and AA, respectively.

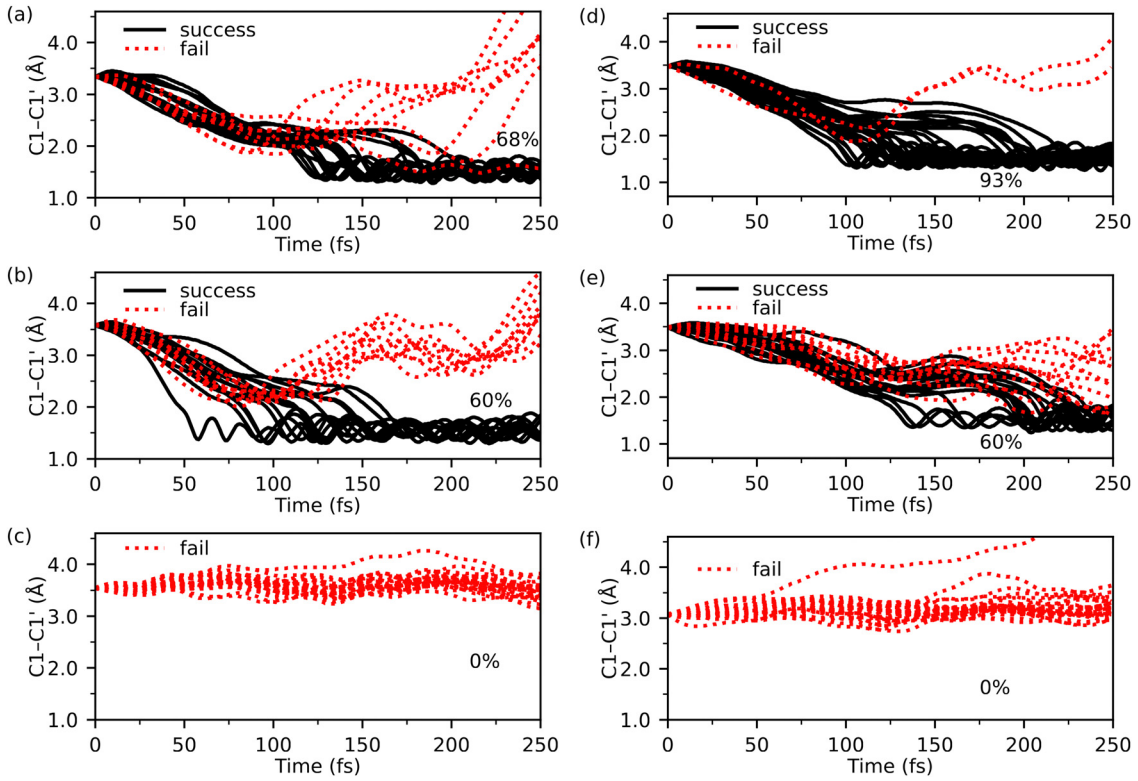

Fig. 4 Changes in C1–C1′ distances during the NAMD trajectories of switches (a) T-**I**, (b) P-**II**, (c) **8**, (d) **10**, (e) **11** and (f) **17** compiled from our previous studies.[39,49] Percentage values refer to the proportion of trajectories that complete photocyclization within 250 fs.

cation in **17**; see Scheme 3b),[49] was found not to undergo photocyclization, as can be seen in Fig. 4 (panels c and f). Specifically, this is because their π-linkers attain excited-state aromaticity upon photoexcitation, as can be inferred from the reversal in the sign of the scaled $\langle NICS_{zz} \rangle$ values from positive to negative in Fig. 3. Overall, excited-state antiaromaticity (aromaticity) of the π-linker is a desirable (undesirable) feature to accomplish high photochemical reactivity.

Despite the relatively large photocyclization efficiencies (60–93%) of **1**, **10** and **11** predicted by simulations,[32,39,49] the actual quantum yields realizable in solution is limited by the fact that the ring-open form exists in two distinct conformations in solution, of which only the anti-parallel conformation (with the central hexatriene moiety adapting a C_2 symmetry) undergoes photocyclization.[36,37] As the two conformers typically have nearly equal energies,[26,30,32] observed quantum yields cannot exceed 50%. However, by introducing intramolecular interactions between the π-linker and an azole-based diaryl core, the photoreactive anti-parallel conformer can be stabilized and high quantum yields of 80–100% are feasible.[33,36–38,42,46,47] For example, by combining a benzoheteroarene π-linker, such as benzothiophene, with a dithiazolyl core as in **13**, the anti-parallel conformer is stabilized by CH···N and S···N interactions, and quantum yields of nearly 100% were reported.[36–38] Interestingly, switches of this type exhibited low photocycloreversion quantum yields of less than 1%,[36–38] possibly because the conical intersection involved in the process is connected to both the ring-open and the ring-closed isomer, but is more geometrically proximate to the latter.[39,49,65]

In addition to high photocyclization quantum yields, another desirable property is high fatigue resistance, which is the ability to switch reversibly between ring-open and ring-closed forms for a large number of cycles. In this regard, a well-known source of poor fatigue resistance in diarylethenes is the transformation of the ring-closed isomer into an annulated bis(dihydro-thiopyran) side-product (**15s**) upon UV irradiation,[34,66,67] as depicted in Scheme 4 for the dithienylbiphenylene switch **15**, considered in our recent work.[34] Commonly used strategies to suppress the formation of the side-product include carrying out irradiation in the solid state,[34] or employing triplet sensitizers such as diacetyl to induce photocyclization in the lowest triplet state of the switch.[68] Alternatively, it was observed that replacing the dithienyl core in **15** with dithiazolyl core in **16** completely suppresses the formation of the side-product, and also improves the photostability.[34] Overall, it can be concluded that replacing the dithienyl core with a dithiazolyl core in switches containing polycyclic aromatic π-linkers is a promising strategy to improve both photoreactivity and fatigue resistance.

Besides inducing formation of the side-product from the ring-closed form of diarylethenes, UV light also causes photo-oxidation and photodegradation of switches over time.[66,67] Therefore, it is desirable to tune optical properties of these switches to ensure that photocyclization can be induced by less

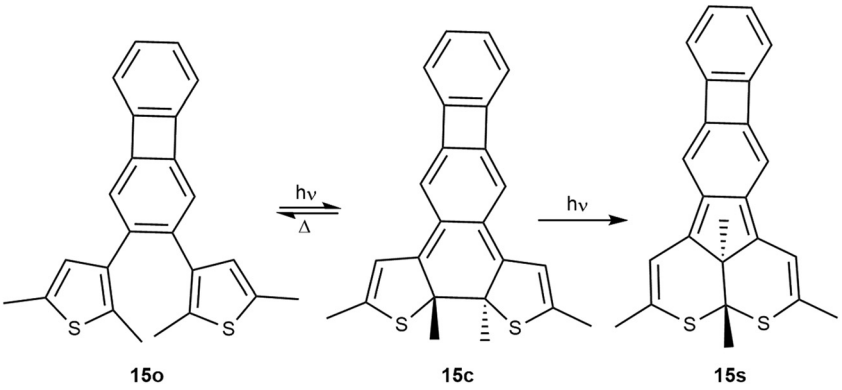

Scheme 4 Possible side reaction that hampers the fatigue resistance of **15**.

damaging visible light.[69,70] To date, studies on the visible-light-activation of diarylethenes have primarily focused on P-type switches,[69,70] employing two distinct strategies. A common approach involves reducing the HOMO–LUMO energy gap of the ring-open form of the switch through extending π-conjugation either in the diaryl core[71–73] or in the π-linker.[74] For example, introducing perylene-based dyes at one of the reactive carbons (C2 and C2′) of the diaryl core significantly red-shifted the absorption band of the ring-open form, with λ_{max} values around 550 nm.[71] Similarly, employing cyanine-based dyes at the lateral carbons (C5 and C5′) enabled visible-light-activated photocyclization at irradiation wavelengths of around 400 nm.[72] However, these modifications resulted in low photocyclization quantum yields,[71,72] or in some cases led to a complete loss of photoswitching behavior.[71] In contrast, introducing a heteroaromatic thieno[3,2-*b*]phosphole oxide π-linker lead to high quantum yields for both photocyclization (0.87) and photocycloreversion (0.44), upon irradiation with violet and green light, respectively.[74] Owing to aromaticity of the π-linker, such systems might also exhibit T-type switching behavior.

Another approach to achieve visible-light photoswitching in diarylethenes involves the use of triplet sensitizers,[34,68] which absorb in visible region and induce photocyclization typically by triplet energy transfer to the diarylethene unit. Conventionally, transition metal complexes have been employed as sensitizers,[75–77] which often result in low photocyclization quantum yields.[75–77] In recent years, metal-free organic sensitizers such as xanthone,[78] phenanthrene,[78] pyrene,[78] and biacetyl[34,68] have been explored, either by direct mixing with the diarylethene unit[34,78] or by covalently linking the sensitizer to the diaryl core.[68] However, organic sensitizers generally exhibit large singlet–triplet energy gaps and weak absorption in the visible region,[69,70] necessitating a large excess of sensitizer for efficient photoswitching.[69,70] To address these limitations, sensitizers with narrow singlet–triplet energy gaps – such as thermally-activated delayed fluorescence (TADF) systems[79,80] and quantum dots (QDs)[81,82] – have recently been developed and found to be highly efficient for enabling visible-light-activated photoswitching in both directions. Notably, a single CdS QD was shown to activate at least 18 diarylethene molecules anchored on its surface upon visible-light irradiation.[82]

Stimulus-induced energy release

For practical realization of MOST potential of T-type diarylethenes, controlled release of stored energy by application of an appropriate external stimulus is critical. While large thermal cycloreversion barriers and low photocycloreversion quantum yields ensure long-term energy storage without spontaneous dissipation under ambient conditions, the ability to lower the cycloreversion barriers through catalysis is essential to make these switches functional. In this regard, the presence of a heteroarene unit containing a basic nitrogen atom is beneficial, as it renders these systems responsive to acid catalysis.[7,64,83–85] Specifically, it has been demonstrated that protonation of the nitrogen atom in DAHs (such as **6**), using trilfluoroacetic acid, accelerates cycloreversion by several orders of magnitude.[83,84] This acceleration has been attributed to the electron-withdrawing effect of the protonated sites, which destabilizes the ring-closed form.[7,83–85] A recent study investigating the effect of solvent polarity on the cycloreversion kinetics of DABs found that polar protic solvents lower the cycloreversion barrier in a DAB switch bearing *p*-methoxy groups on lateral phenyl substituents at the C5 and C5′ atoms of the diaryl core (see Scheme 2), by about 8 kJ mol^{-1}.[86] Moreover, addition of trilfluoroacetic acid further accelerated cycloreversion by protonating oxygen atoms of the methoxy substituents.[86]

Interestingly, it was demonstrated that a typical P-type diarylethene featuring a fluorenol moiety on the diaryl core can be made to function as a T-type diarylethene by acid catalysis using triflic acid, which reduced cycloreversion barrier by a substantial 57 kJ mol^{-1}.[8] Such significant acceleration resulted from protonation of the hydroxy group of fluorenol, followed by dehydration to generate an antiaromatic fluorenyl cation.[8] Thus, the presence of Lewis basic sites or substituents in diarylethenes provides a means to control heat release through acid-gated photochromism.[7,8,64,83–86] Alternatively, electrochemical oxidation has been demonstrated to offer high cycloreversion rates and exceptionally large current conversion

efficiencies (up to 900%) in DAHs **6** and **7**.[9,10] This is because the cycloreversion reaction, albeit initiated by an applied potential, is sustained by a chain reaction between the oxidized ring-open form and the non-oxidized ring-closed form.[9,10]

Summary and outlook

In this perspective article, we have shown how T-type diarylethenes can be made into promising materials for solar energy storage through careful tuning of their aromatic features in both ground and excited states. Through a systematic analysis of computational and experimental data compiled from several studies,[31–34,38,39,45,48,49] we have discussed how aromaticity of the π-linker can be used as a design principle in formulating three distinct strategies to modulate thermal and photochemical reactivity of T-type diarylethenes to develop them into MOST systems. First, reducing the aromaticity of a monocyclic π-linker (relative to benzene) in the ring-open form of the switch induces a destabilizing effect both in the ring-open and TS forms relative to the corresponding ring-closed form, resulting in improved thermal stability of the latter and yielding large thermal cycloreversion barriers at the cost of reduced energy-storage densities.[31–33,45] Second, the ring-closed form can also be stabilized by increasing the aromaticity of its π-linker. This has been accomplished by employing in the ring-open form a polycyclic bridge with multiple aromatic rings,[34,48,49] of which aromaticity of the terminal ring might get amplified upon photocyclization.[34,49] Third, in both of the aforementioned types of T-type diarylethenes – those with reduced aromaticity in a monocyclic π-linker in the ring-open form and those with increased aromaticity in one of the rings of a polycyclic π-linker in the ring-closed form – high photocyclization reactivity of the anti-parallel conformer of the ring-open form is feasible due to the onset of excited-state antiaromaticity of the π-linker upon electronic excitation of the switch.[39,49] However, translating this promising feature into high photocyclization quantum yields in solution requires replacing the dithienyl core of these switches with the dithiazolyl core, which enhances the population of the photoreactive anti-parallel conformer.[33,36–38,42,46,47]

Several challenges still remain to be addressed for practical utility of T-type diarylethenes in MOST applications. First, tuning absorption properties of these switches from the UV to the visible regime without impacting other important MOST criteria, such as high photocyclization quantum yields and large energy-storage densities, still remains a largely unexplored avenue. Second, achieving both large rates and efficiencies in heat release by stimulus-induced cycloreversion presents a considerable challenge, as approaches like electrochemical oxidation may lead to electrode fouling and undesirable side reactions.[87] Finally, integrating these systems into functional MOST devices demands that their photoswitching properties are preserved even after incorporation into complex device architectures. In this regard, diarylethenes appear promising due to their efficient solid-state switching[26,81,82] and their ability to anchor onto surfaces of quantum dots,[81,82] which facilitate convenient fabrication and seamless integration into scalable solid-state MOST devices.

Data availability

No primary research results, software or code have been included and no new data were generated or analysed as part of this perspective article.

Conflicts of interest

The authors declare no conflict of interest.

Acknowledgements

B. O. acknowledges financial support by the Department of Science and Technology (DST), New Delhi, India, under a DST SERB-SURE scheme (grant SUR/2022/001766). B. D. acknowledges financial support by the Swedish Research Council (grant 2019-03664), the Olle Engkvist Foundation (grant 204-0183) and the Carl Trygger Foundation (grants CTS 20:102 and CTS 21:1545). Dr K. N. thanks to SRM university for providing startup grant (SRMAP/URG/SEED/2023-24/028). T. S. acknowledges financial support by SRM University-AP. The computations were enabled by resources provided by SRM University-AP, and by the National Academic Infrastructure for Supercomputing in Sweden (NAISS) and the Swedish National Infrastructure for Computing (SNIC) at the National Supercomputer Centre partially funded by the Swedish Research Council (grants 2022-06725 and 2018-05973).

References

1 A. Malhotra, B. Battke, M. Beuse, A. Stephan and T. Schmidt, *Renewable Sustainable Energy Rev.*, 2016, **56**, 705–721.
2 B. R. de Vasconcelos and J.-M. Lavoie, *Front. Chem.*, 2019, **7**, 392.
3 T. J. Kucharski, Y. Tian, S. Akbulatov and R. Boulatov, *Energy Environ. Sci.*, 2011, **4**, 4449–4472.
4 C. Sun, C. Wang and R. Boulatov, *ChemPhotoChem*, 2019, **3**, 268–283.
5 Z. Wang, H. Hölzel and K. Moth-Poulsen, *Chem. Soc. Rev.*, 2022, **51**, 7313–7326.
6 K. Moth-Poulsen, D. Ćoso, K. Börjesson, N. Vinokurov, S. K. Meier, A. Majumdar, K. P. C. Vollhardt and R. A. Segalman, *Energy Environ. Sci.*, 2012, **5**, 8534–8537.
7 L. Chocron, N. Baggi, E. Ribeiro, V. Goetz, P. Yu, K. Nakatani and R. Métivier, *Chem. Sci.*, 2024, **15**, 16034–16039.
8 J. Gurke, M. Quick, N. P. Ernsting and S. Hecht, *Chem. Commun.*, 2017, **53**, 2150–2153.
9 J. P. Calupitan, T. Nakashima, Y. Hashimoto and T. Kawai, *Chem. – Eur. J.*, 2016, **22**, 10002–10008.

10 T. Nakashima, Y. Kajiki, S. Fukumoto, M. Taguchi, S. Nagao, S. Hirota and T. Kawai, *J. Am. Chem. Soc.*, 2012, **134**, 19877–19883.
11 A. Lennartson, A. Roffey and K. Moth-Poulsen, *Tetrahedron Lett.*, 2015, **56**, 1457–1465.
12 Z. Wang, P. Erhart, T. Li, Z.-Y. Zhang, D. Sampedro, Z. Hu, H. A. Wegner, O. Brummel, J. Libuda, M. B. Nielsen and K. Moth-Poulsen, *Joule*, 2021, **5**, 3116–3136.
13 M. H. Hansen, J. Elm, S. T. Olsen, A. N. Gejl, F. E. Storm, B. N. Frandsen, A. B. Skov, M. B. Nielsen, H. G. Kjaergaard and K. V. Mikkelsen, *J. Phys. Chem. A*, 2016, **120**, 9782–9793.
14 M. Jevric, A. U. Petersen, M. Mansø, S. Kumar Singh, Z. Wang, A. Dreos, C. Sumby, M. B. Nielsen, K. Börjesson, P. Erhart and K. Moth-Poulsen, *Chem. – Eur. J.*, 2018, **24**, 12767–12772.
15 Z. Wang, A. Roffey, R. Losantos, A. Lennartson, M. Jevric, A. U. Petersen, M. Quant, A. Dreos, X. Wen, D. Sampedro, K. Börjesson and K. Moth-Poulsen, *Energy Environ. Sci.*, 2019, **12**, 187–193.
16 F.-Y. Meng, I.-H. Chen, J.-Y. Shen, K.-H. Chang, T.-C. Chou, Y.-A. Chen, Y.-T. Chen, C.-L. Chen and P.-T. Chou, *Nat. Commun.*, 2022, **13**, 797.
17 E. M. Arpa and B. Durbeej, *Chem. Methods*, 2023, **3**, e202200060.
18 V. Caia, G. Cum, R. Gallo, V. Mancini and E. Pitoni, *Tetrahedron Lett.*, 1983, **24**, 3903–3904.
19 W. Moormann, T. Tellkamp, E. Stadler, F. Röhricht, C. Näther, R. Puttreddy, K. Rissanen, G. Gescheidt and R. Herges, *Angew. Chem., Int. Ed.*, 2020, **59**, 15081–15086.
20 J.-F. Xu, Y.-Z. Chen, L.-Z. Wu, C.-H. Tung and Q.-Z. Yang, *Org. Lett.*, 2013, **15**, 6148–6151.
21 J. Mogensen, O. Christensen, M. D. Kilde, M. Abildgaard, L. Metz, A. Kadziola, M. Jevric, K. V. Mikkelsen and M. B. Nielsen, *Eur. J. Org. Chem.*, 2019, 1986–1993.
22 M. Jevric, Z. Wang, A. U. Petersen, M. Mansø, C. J. Sumby, M. B. Nielsen and K. Moth-Poulsen, *Eur. J. Org. Chem.*, 2019, 2354–2361.
23 K. Morimitsu, K. Shibata, S. Kobatake and M. Irie, *J. Org. Chem.*, 2002, **67**, 4574–4578.
24 K. Edel, X. Yang, J. S. A. Ishibashi, A. N. Lamm, C. Maichle-Mössmer, Z. X. Giustra, S. Liu and H. F. Bettinger, *Angew. Chem., Int. Ed.*, 2018, **57**, 5296–5300.
25 K. Börjesson, D. Ćoso, V. Gray, J. C. Grossman, J. Guan, C. B. Harris, N. Hertkorn, Z. Hou, Y. Kanai, D. Lee, J. P. Lomont, A. Majumdar, S. K. Meier, K. Moth-Poulsen, R. L. Myrabo, S. C. Nguyen, R. A. Segalman, V. Srinivasan, W. B. Tolman, N. Vinokurov, K. P. C. Vollhardt and T. W. Weidman, *Chem. – Eur. J.*, 2014, **20**, 15587–15604.
26 M. Irie, T. Fukaminato, K. Matsuda and S. Kobatake, *Chem. Rev.*, 2014, **114**, 12174–12277.
27 A. G. Lvov, M. M. Khusniyarov and V. Z. Shirinian, *J. Photochem. Photobiol., C*, 2018, **36**, 1–23.
28 K. Yuan, J. Boixel, H. L. Bozec, A. Boucekkine, H. Doucet, V. Guerchais and D. Jacquemin, *Chem. Commun.*, 2013, **49**, 7896–7898.
29 A. G. Lvov, A. M. Kavun, V. V. Kachala, Y. V. Nelyubina, A. V. Metelitsa and V. Z. Shirinian, *J. Org. Chem.*, 2017, **82**, 1477–1486.
30 M. Mörtel, A. Witt, F. W. Heinemann, S. Bochmann, J. Bachmann and M. M. Khusniyarov, *Inorg. Chem.*, 2017, **56**, 13174–13186.
31 D. Kitagawa, T. Nakahama, Y. Nakai and S. Kobatake, *J. Mater. Chem. C*, 2019, **7**, 2865–2870.
32 B. Oruganti, P. P. Kalapos, V. Bhargav, G. London and B. Durbeej, *J. Am. Chem. Soc.*, 2020, **142**, 13941–13953.
33 S. Hamatani, D. Kitagawa and S. Kobatake, *J. Phys. Chem. C*, 2021, **125**, 4588–4594.
34 P. P. Kalapos, P. J. Mayer, T. Gazdag, A. Demeter, B. Oruganti, B. Durbeej and G. London, *J. Org. Chem.*, 2022, **87**, 9532–9542.
35 V. B. Kharitonov, E. S. Sergeeva, E. K. Kouame, Y. V. Nelyubina, I. A. Ushakov, D. A. Loginov and A. G. Lvov, *Org. Lett.*, 2022, **24**, 7538–7543.
36 S. Fukumoto, T. Nakashima and T. Kawai, *Angew. Chem., Int. Ed.*, 2011, **50**, 1565–1568.
37 R. Li, T. Nakashima, O. Galangau, S. Iijima, R. Kanazawa and T. Kawai, *Chem. – Asian J.*, 2015, **10**, 1725–1730.
38 R. Asato, C. J. Martin, T. Nakashima, J. P. Calupitan, G. Rapenne and T. Kawai, *J. Phys. Chem. Lett.*, 2021, **12**, 11391–11398.
39 B. Oruganti, J. Wang and B. Durbeej, *J. Org. Chem.*, 2022, **87**, 11565–11571.
40 T. Nakahama, D. Kitagawa and S. Kobatake, *J. Phys. Chem. C*, 2019, **123**, 31212–31218.
41 S. Hamatani, D. Kitagawa, T. Nakahama and S. Kobatake, *Tetrahedron Lett.*, 2020, **61**, 15968–15972.
42 R. Maegawa, D. Kitagawa, S. Hamatani and S. Kobatake, *New J. Chem.*, 2021, **45**, 18969–18975.
43 S. Hamatani, D. Kitagawa, T. Nakahama and S. Kobatake, *Bull. Chem. Soc. Jpn.*, 2023, **96**, 496–502.
44 S. Kawai, T. Nakashima, K. Atsumi, T. Sakai, M. Harigai, Y. Imamoto, H. Kamikubo, M. Kataoka and T. Kawai, *Chem. Mater.*, 2007, **19**, 3479–3483.
45 J. V. Milić, C. Schaack, N. Hellou, F. Isenrich, R. Gershoni-Poranne, D. Neshchadin, S. Egloff, N. Trapp, L. Ruhlmann, C. Boudon, G. Gescheidt, J. Crassous and F. Diederich, *J. Phys. Chem. C*, 2018, **122**, 19100–19109.
46 S. Fukumoto, T. Nakashima and T. Kawai, *Eur. J. Org. Chem.*, 2011, 5047–5053.
47 S. Fukumoto, T. Nakashima and T. Kawai, *Dyes Pigm.*, 2012, **92**, 868–871.
48 Y. Yang, Y. Xie, Q. Zhang, K. Nakatani, H. Tian and W. Zhu, *Chem. – Eur. J.*, 2012, **18**, 11685–11694.
49 T. S, D. S. Perumalla, B. Oruganti and B. Durbeej, *ChemPhotoChem*, 2024, **8**, e202300225.
50 M. G. Evans and M. Polanyi, *Trans. Faraday Soc.*, 1938, **34**, 11–24.
51 H. Ottosson, *Nat. Chem.*, 2012, **4**, 969–971.
52 M. Rosenberg, C. Dahlstrand, K. Kilså and H. Ottosson, *Chem. Rev.*, 2014, **114**, 5379–5425.
53 J. Yan, T. Slanina, J. Bergman and H. Ottosson, *Chem. – Eur. J.*, 2023, **29**, e202203748.
54 A. V. Marenich, C. J. Cramer and D. G. Truhlar, *J. Phys. Chem. B*, 2009, **113**, 6378–6396.

55 M. E. Casida and M. Huix-Rotllant, *Annu. Rev. Phys. Chem.*, 2012, **63**, 287–323.
56 B. O. Roos, P. R. Taylor and P. E. M. Siegbahn, *Chem. Phys.*, 1980, **48**, 157–173.
57 K. Andersson, P.-Å. Malmqvist and B. O. Roos, *J. Chem. Phys.*, 1992, **96**, 1218–1226.
58 J. Finley, P.-Å. Malmqvist, B. O. Roos and L. Serrano-Andrés, *Chem. Phys. Lett.*, 1998, **288**, 299–306.
59 T. M. Krygowski and M. K. Cyrański, *Chem. Rev.*, 2001, **101**, 1385–1419.
60 P. V. R. Schleyer, C. Maerker, A. Dransfeld, H. Jiao and N. J. R. van Eikema Hommes, *J. Am. Chem. Soc.*, 1996, **118**, 6317–6318.
61 S. Noorizadeh and E. Shakerzadeh, *Phys. Chem. Chem. Phys.*, 2010, **12**, 4742–4749.
62 M. Barbatti, *Wiley Interdiscip. Rev.:Comput. Mol. Sci.*, 2011, **1**, 620–633.
63 E. Tapavicza, G. D. Bellchambers, J. C. Vincent and F. Furche, *Phys. Chem. Chem. Phys.*, 2013, **15**, 18336–18348.
64 T. Sukumar, M. K. Ravva and B. Oruganti, *J. Org. Chem.*, 2025, **90**, 2770–2782.
65 J. Wang, T. Sukumar, D. S. Perumalla, B. Oruganti and B. Durbeej, *ChemPhotoChem*, 2025, e202400418, DOI: **10.1002/cptc.202400418**.
66 D. Mendive-Tapia, A. Perrier, M. J. Bearpark, M. A. Robb, B. Lasorne and D. Jacquemin, *Phys. Chem. Chem. Phys.*, 2014, **16**, 18463–18471.
67 M. Herder, B. M. Schmidt, L. Grubert, M. Pätzel, J. Schwarz and S. Hecht, *J. Am. Chem. Soc.*, 2015, **137**, 2738–2747.
68 S. Fredrich, R. Göstl, M. Herder, L. Grubert and S. Hecht, *Angew. Chem., Int. Ed.*, 2016, **55**, 1208–1212.
69 D. Bléger and S. Hecht, *Angew. Chem., Int. Ed.*, 2015, **54**, 11338–11349.
70 Z. Zhang, W. Wang, M. O'Hagan, J. Dai, J. Zhang and H. Tian, *Angew. Chem., Int. Ed.*, 2022, **61**, e202205758.
71 T. Fukaminato, T. Hirose, T. Doi, M. Hazama, K. Matsuda and M. Irie, *J. Am. Chem. Soc.*, 2014, **136**, 17145–17154.
72 F. Hu, M. Cao, X. Ma, S. H. Liu and J. Yin, *J. Org. Chem.*, 2015, **80**, 7830–7835.
73 T. Sumi, T. Kaburagi, M. Morimoto, K. Une, H. Sotome, S. Ito, H. Miyasaka and M. Irie, *Org. Lett.*, 2015, **17**, 4802–4805.
74 N. M.-W. Wu, M. Ng, W. H. Lam, H.-L. Wong and V. W.-W. Yam, *J. Am. Chem. Soc.*, 2017, **139**, 15142–15150.
75 V. W.-W. Yam, C.-C. Ko and N. Zhu, *J. Am. Chem. Soc.*, 2004, **126**, 12734–12735.
76 M. T. Indelli, S. Carli, M. Ghirotti, C. Chiorboli, M. Ravaglia, M. Garavelli and F. Scandola, *J. Am. Chem. Soc.*, 2008, **130**, 7286–7299.
77 W. Tan, Q. Zhang, J. Zhang and H. Tian, *Org. Lett.*, 2009, **11**, 161–164.
78 R. Murata, T. Yago and M. Wakasa, *J. Phys. Chem. A*, 2015, **119**, 11138–11145.
79 Z. Zhang, J. Zhang, B. Wu, X. Li, Y. Chen, J. Huang, L. Zhu and H. Tian, *Adv. Opt. Mater.*, 2018, **6**, 1700847.
80 Z. Zhang, W. Wang, P. Jin, J. Xue, L. Sun, J. Huang, J. Zhang and H. Tian, *Nat. Commun.*, 2019, **10**, 4232.
81 L. Hou, W. Larsson, S. Hecht, J. Andréasson and B. Albinsson, *J. Mater. Chem. C*, 2022, **10**, 15833–15842.
82 K. Chen, J. Liu, J. Andréasson, B. Albinsson, T. Liu and L. Hou, *Chem. Sci.*, 2024, **15**, 20365–20370.
83 C. Coudret, T. Nakagawa, T. Kawai and J.-C. Micheau, *New J. Chem.*, 2009, **33**, 1386–1392.
84 T. Nagakawa, C.-L. Serpentini, C. Coudret, J.-C. Micheau and T. Kawai, *Dyes Pigm.*, 2011, **89**, 271–277.
85 Y. Kutsunugi, C. Coudret, J. C. Micheau and T. Kawai, *Dyes Pigm.*, 2012, **92**, 838–846.
86 Y. Morimoto, D. Kitagawa, S. Hamatani and S. Kobatake, *Chem. Lett.*, 2024, **53**, upad023.
87 F. Hemauer, H.-P. Steinrück and C. Papp, *ChemPhysChem*, 2024, **25**, e202300806.

